RESEARCH FOR JET FLOW INFLUENCES TO WING-MOUNTED CIVIL AIRCRAFT AERODYNAMIC CHARACTERISTICS

Tan Zhaoguang, Chen Yingchun, Huang wei
Shanghai Aircraft Design and Research Institute,
Commercial Aircraft Corporation of China, Shanghai, China
tanzhaoguang@comac.cc

Keywords: *jet flow; wing-mounted civil aircraft; CFD*

Abstract

The numerical simulation of the aerodynamic characteristics influences for civil wing-mounted jet exhausts were presented. Three-dimensional time-dependent compressible Reynolds-averaged Navier-Stokes equations were solved with third-order upwind-biased flux-difference splitting method and approximate factorization method. The point-to-point patched multi-block technology was used to generate high quality grid. The multi-grid technique was employed to accelerate the convergence. For a better simulation of the power effects, the fan inlet face boundary conditions and jet-exit boundary conditions were determined. Computational results and comparisons with experimental data are presented. The good agreement indicates that the numerical methods are validated. From the results, lift and moment characteristics are influenced by jet exhausts certainly.

1 General Introduction

Modern civil aircrafts often use Wing-mounted configuration. This configuration has many advantages, such as engines can unload the wing structure in flights and damp wing vibration in turbulent air flow, noise level of passenger cabin is lower than most of the other configurations. This configuration can ease the maintenance and replacement of engines [1]. However, Wing-mounted configuration also has some defects. From aerodynamics, one of these defects is the existent of engines and exhaust jet flow which makes the flow field around the wing and horizontal tail complicated. Practices have proved that the engine and exhaust flow affect the aerodynamic performance of civil aircraft obviously. Exhaust jet flow has induced effect to around flow field, enables aircraft flow velocity and direction changes in local, thereby causes the wing, horizontal tail and other parts of aircraft aerodynamic characteristics change [2]. Therefore, to predict the engine jet flow on aircraft exterior flow field interference effects is very necessary for evaluating and improving the aerodynamic performance, stability and control performance, and also important to aircraft/engine integrated design.

Wind tunnel tests have been utilized widely to evaluate exhaust jet flow influence to wing-mounted civil aircraft aerodynamic characteristics. But Wind tunnel tests need very high technique to carry out, and the costs are high. As the development of Computational Fluid Dynamic (CFD), using the numerical calculation method on the exhaust flow impact assessment has become more and more convenient. This paper focuses on studies using the Navier-Stokes equations to conduct this research.

2 The control equations and discrete scheme

This paper adopted the control equation for three dimensional Reynolds averaged integral form N-S equations.

$$\frac{\partial}{\partial t}\iiint \boldsymbol{Q}\,dv+\iint_s \boldsymbol{f}\,\boldsymbol{n}\,ds=0 \qquad (1)$$

Among them, v is the control volume, s is the control of body surface, $\boldsymbol{Q}$ is conserved quantities, $\boldsymbol{f}$ is the sum of inviscid fluxes and viscous flux via surface s, and $\boldsymbol{n}$ is the normal unit vectors of the outer surfaces. Space semi-discrete scheme is constructed base on the finite volume method. The inviscid fluxes are discretized with upwind flux-difference splitting method (FDS), and the viscous fluxes are discretized with second-order central differences. The calculation is advanced in time with the implicit approximate factorization (AF) method. SA turbulence model is adopted.

3 The engine intake and exhaust boundary conditions

In this paper, characteristic line theory was used to construct non reflecting boundary condition in the far field boundary; the no-slip, adiabatic wall and the zero pressure gradient conditions were used in the body surface; block junction boundary used multiple point to point overlapping grid, so only in the lap surface used virtual grid technology to achieve physical quantity transfer, to ensure the conservation of flux. The conventional methods to deal with the boundary condition are shown in references [3]. This paper focused on how to use unified pattern by setting the inlet, outlet boundary condition to simulate engine powered effects in the aircraft/propulsion integration analysis process [4].

3.1 The fan inlet boundary conditions

In the fan inlet boundary, blades rotate all times, the real boundary condition is very complex, so it needs to be simplified. Mass flow, pressure or velocity can be given to the simplified fan inlet boundary conditions, and then use some relationship equations to calculate the other boundary conditions, such as temperature, density and so on.

Inlet mass flow ratio can be expressed as:

$$\dot{m}_{fan}=\rho_{fan}q_{fan}A_{fan}=\rho_{\infty}q_{\infty}A_{\infty} \qquad (2)$$

Where A_{HL} is the leading edges of the cross sectional area of the nacelle, A_{fan} is the fan surface area.

By the next relation, mass flow ratio can be denoted through constant entropy and energy conservation using the fan surface Mach number M_f and the far field Maher number M_∞:

$$M.F.R.=\frac{A_{fan}}{A_{HL}}.M_f.(1+\frac{\gamma-1}{2}M_f^2)^{-\frac{\gamma+1}{2(\gamma-1)}}.\frac{\rho_0}{\rho_\infty}.\frac{a_0}{q_\infty} \qquad (3)$$

where: $\frac{a_0}{q_\infty}=(\frac{\gamma-1}{2}+\frac{1}{M_\infty^2})^{\frac{1}{2}}$

$$\frac{\rho_0}{\rho_\infty}=(1+\frac{\gamma-1}{2}M_\infty^2)^{\frac{1}{\gamma-1}}$$

From above, M_f can be obtained, and then ρ_{fan}, T_{fan}, q_{fan}, p_{fan} can be calculated through the isentropic relations and sonic formula. Through these parameters, the fan inlet surface boundary conditions are defined.

3.2 The nozzle boundary conditions

Inlet mass flow is divided into fan jet flow and turbo jet flow when a real engine working. Fuel is added to the turbine jet, but in a turbofan engine, the fuel flow rate is fairly small, so it can be neglected. Thus bypass ratio (*B.R.*) can be used to the fan jet flow and jet flow turbine definition. Fan jet flow Mach number (M_F) can be determined with the same method in fan inlet:

$$M.F.R.=\frac{A_{FEX}}{A_{HL}}\cdot\frac{1+B.R.}{B.R.}\cdot\frac{F.P.R.}{\sqrt{F.T.R.}}\cdot M_{FEX}$$
$$\cdot(1+\frac{\gamma-1}{2}M_{FEX}^2)^{-\frac{\gamma+1}{2(\gamma-1)}}\cdot\frac{\rho_0}{\rho_\infty}\cdot\frac{a_0}{q_\infty} \qquad (4)$$

In (4), *F.P.R.* is the fan jet flow total pressure ratio ($p_{0F}/p_{0\infty}$), F.T.R. is the total temperature ratio ($T_{0F}/T_{0\infty}$), A_{FEX} is the fan jet outlet area. Various boundary conditions of fan jet flow can be obtained through (4) and the gas state equation, sonic formula, isentropic relations.

Turbo jet flow boundary conditions can be concluded in the similar way to fan jet flow.

4 Computational methods verification

In order to validate the boundary condition processing method, grid generation and flow field calculation method were correct, an isolated engine model and the DLR-F6 model were numerically simulated, and compared with the experimental results.

4.1 Isolated engine flow field numerical simulation

4.1.1 The geometry model and mesh generation

The isolated engine adopted in this paper is an axisymmetric model of turbofan engine, taken from the Japanese Aerospace Technology Research Institute" NAL-AERO-02-01" T.P.S (Turbine Powered Simulation) wind tunnel experiment model [5]. The reference provides the two-dimension half model data (Fig. 1), and then used the modeling software to build the three-dimensional model.

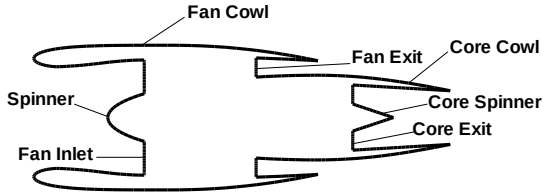

Fig. 1. " NAL-AERO-02-01" T.P.S. Experimental model of meridian plane

In this paper, the multi block structure grid was used (Fig. 2). In the near surface area used "O" type grid, which can guarantee a good near surface grid orthogonality, and very suitable for the simulation of aircraft boundary layer flow. In the field of other regions use "H" type grid.

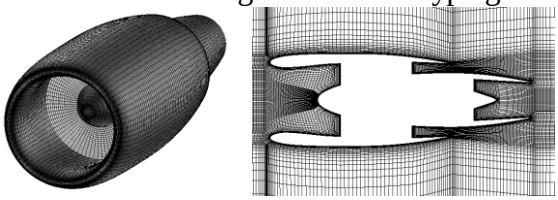

Fig.2" NAL-AERO-02-01" T.P.S. Model mesh

4.1.2 Calculation results and analysis

The intake and exhaust flow field under two different working conditions (shown in Tab. 1) were numerically simulated and analyzed (Reynold numbers are 1×10^6, based on the engine maximum diameter).

Tab. 1. The case parameters

Parameters	Case 1	Case 2
M_∞	0.8008	0.6024
α	0.0 °	0.0 °
M.F.R.	0.4973	0.4961
F.P.R.	1.3428	1.2052
F.T.R.	1.1086	1.0634
C.P.R.	0.0617	0.1003
C.T.R.	0.6907	0.7480

The calculated values and experimental values of fan and core cowl surface pressure distribution under the two different working conditions are compared in Fig. 3. Calculated values are consistent with the experimental values well. From the Mach number contour (Fig. 4) the jet effect can be seen visually. It can be proved that the numerical simulation for isolated engine, grid strategy and intake, exhaust boundary processing method are suitable.

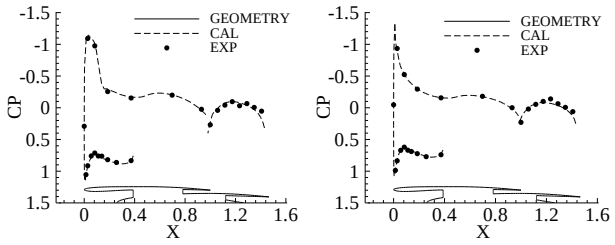

(a) Case 1 (b) Case 2

Fig. 3. Surface pressure comparing between calculated and experimental values

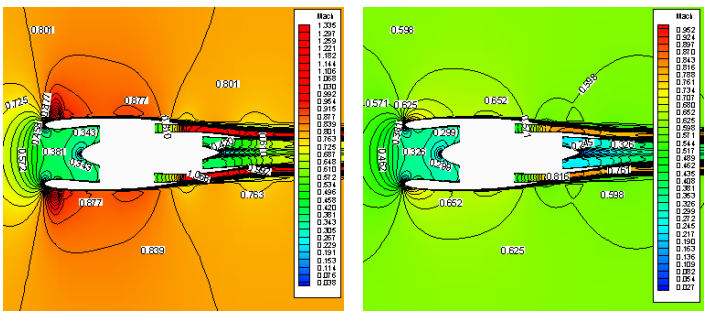

(a) Case 1 (b) Case 2

Fig. 4. Meridian plane Mach number contour

4.2 DLR-F6 flow field numerical simulation

4.2.1 Geometric model and computational grid

In order to validate the numerical method farther, DLR-F6 model was also simulated numerically in this paper. DLR-F6 model is a twin-engined wide-body aircraft, there are varieties of wind tunnel experiment and numerical calculation method verification have been carried on it over the years. Fig. 5 is the DLR-F6 wing-body/pylon/nacelle (WBPN) space grid graph.

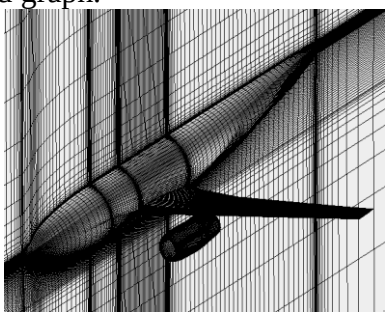

Fig. 5. DLR-F6 wing-body/pylon/nacelle grid

4.2.2 Calculation results and analysis

The DLR-F6 wing surface pressure distribution compare between calculated value and experimental value (M=0.75,α=1.23 °;Reynolds number is 3×10^6, based on the mean aerodynamic chord) are shown in Fig. 6. And the DLR-F6 nacelle surface pressure distribution compare between calculated value and experimental value (M=0.75, α=1.23 °) are shown in Fig. 7. The calculation results are in excellent agreement with experiment at every stations, it show that the grid generation strategy and numerical calculation method are suitable.

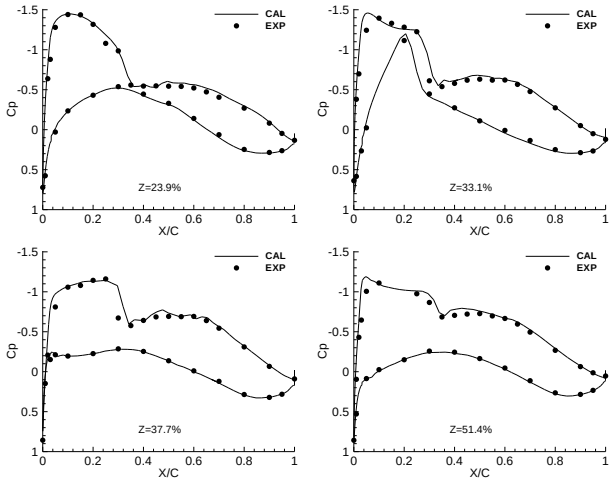

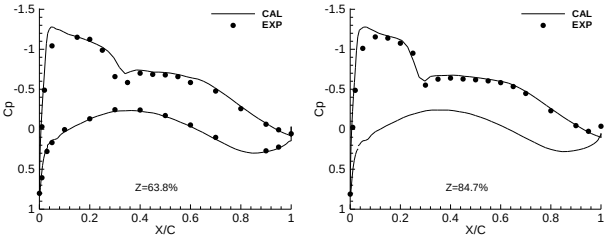

Fig. 6. DLR-F6 wing surface pressure distribution (M = 0.75, α= 1.23 °)

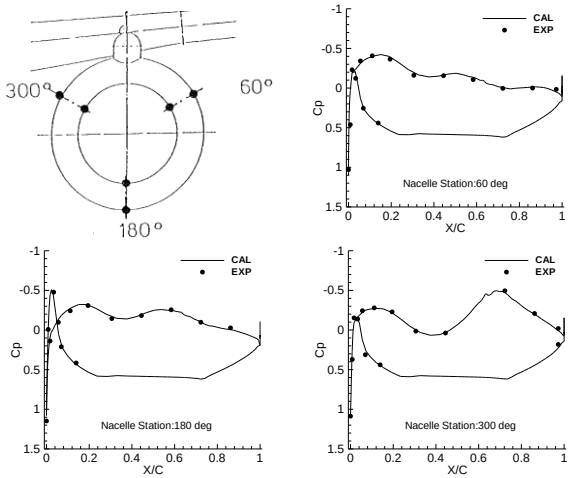

Fig. 7. Nacelle surface pressure distribution at different stations (M = 0.75, α= 1.23 °)

5 Jet flow influences to aircraft aerodynamic characteristics

5.1 Geometric model and computational grid

In this paper, a wing-mounted aircraft cruise configuration was researched. In order to get jet flow influences to the whole aircraft and components, the high speed and low speed aerodynamic characteristics were both calculated. High and low speed respectively used the aircraft cruise and landing power boundary conditions. Fig. 8 shows the grid.

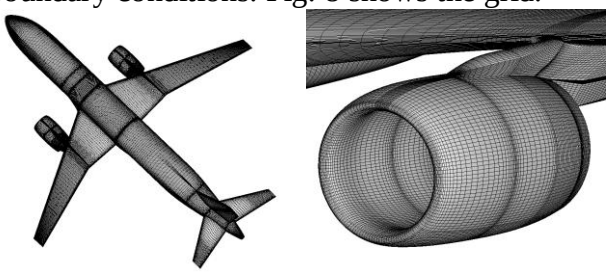

Fig. 8. The aircraft surface grid

5.2 Jet flow influences to wing and tail local flow field

Fig. 9 is the total pressure ratio ($p_0/p_{0\infty}$) contour at M=0.785, α=2.0 °, this figure show the jet flow visually.

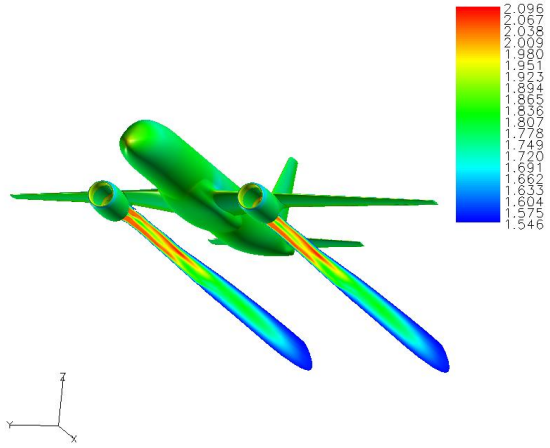

Fig. 9. Total pressure ratio ($p_0/p_{0\infty}$) contour at M=0.785, α=2.0 °

Fig. 10 and Fig. 11 respectively show wing surface pressure distribution comparison between with and without jet flow conditions at different span stations under high and low speed, 32% and 39% are respectively at inside and outside area of the pylon. As can be seen from the graph, jet flow influence to the upper wing surface is small, and influence the lower wing surface severer than the upper wing surface. At the inside and outside position of pylon, interference to the lower wing surface flows are larger.

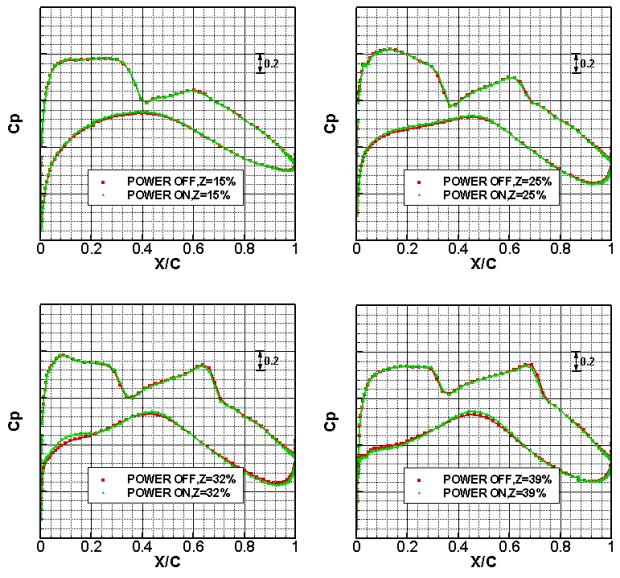

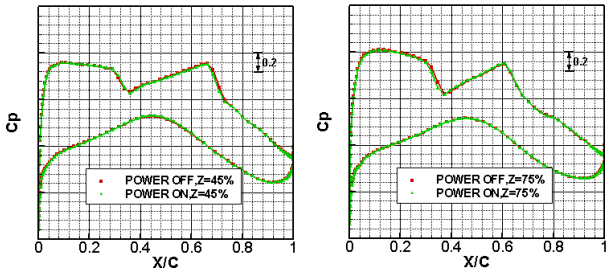

Fig. 10. Wing surface pressure distribution at M=0.785, α=2.0 °

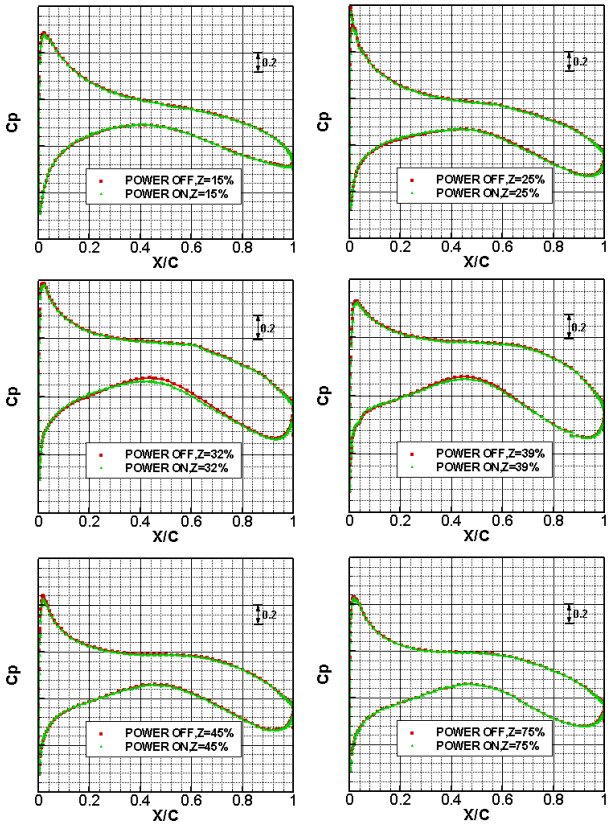

Fig. 11. Wing surface pressure distribution at M=0.20, α=3.0 °

Fig. 12 and Fig. 13 respectively show horizontal tail surface pressure distribution comparison between with and without jet flow conditions at different span stations under high and low speed. It can be seen from the figure that the horizontal tail is also affected by the jet flow, and close to the wingtip position more, interfered more. This is because the jet eject effect weaken the downwash which wing causes, thereby changes the direction of the flow, such as Fig.14, velocity vector contrast at horizontal tail 92% station. It can be seen that jet flow impact velocity direction. And the change from

root to tip gradually becomes larger, because the more close to the tip, the more influences.

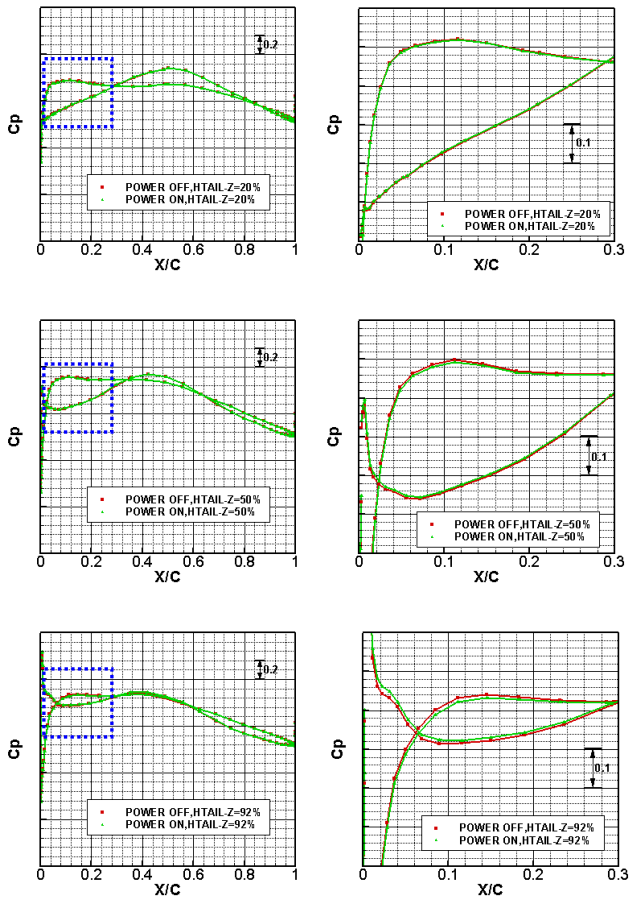

Fig. 12. Horizontal tail surface *Cp* comparison at M=0.785, α=2.0 °(The figures at right are the close-ups of left blue dashed boxes)

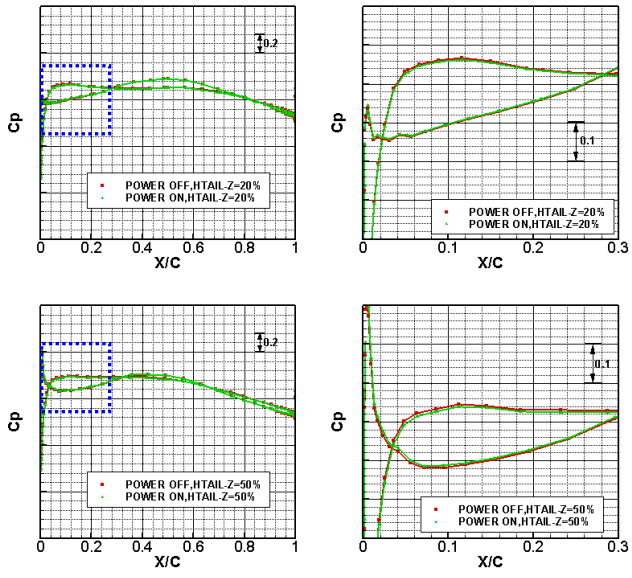

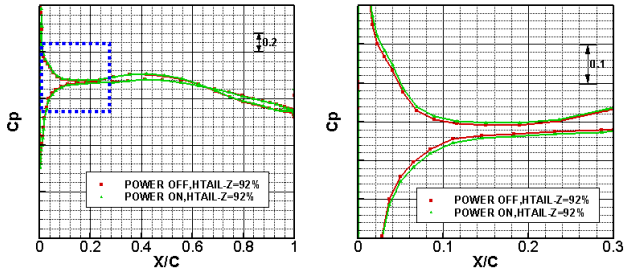

Fig. 13. Horizontal tail surface *Cp* comparison at M=0.20, α=2.0 °(The figures at right are the close-ups of left blue dashed boxes)

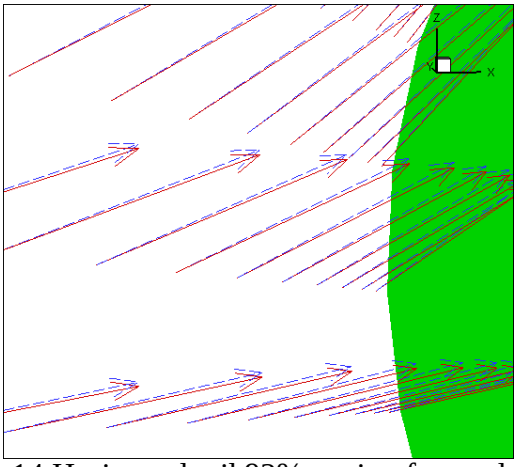

Fig.14 Horizontal tail 92% station front edge velocity vector contrast (Red solid is without jet, blue dotted is with jet)

5.2 Jet flow influences to the aircraft life and moment characteristics

Jet flow influences to the aircraft lift and moment characteristics can be seen from Fig. 15 and Fig. 16.

It can be seen that the lift reduces because of jet effect. When M = 0.785, at cruise angle (about 2 °), lift coefficient (CL) reduces about 0.013 (2.5%); when M = 0.20, a = 3 °, decreases by approximately 0.005 (1%). And jet flow makes the lift line slope has slightly increased, but the change is very small.

At the same time, jet flow makes the aircraft moment decreased. When M = 0.785 in cruising state (CL = 0.55), moment coefficient (CM) decreases about 0.005 (6%); when M = 0.20, CL = 0.6, CM decreases about 0.02 (25%). This is mainly due to the jet ejector effect weakens the downwash which wing causes, thereby the direction of the flow changes. And

the moment line slope is not influenced obviously.

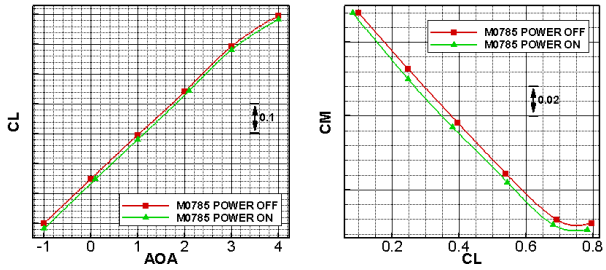

Fig. 15. Jet flow influences to the aircraft life and moment characteristics at *M*=0.785

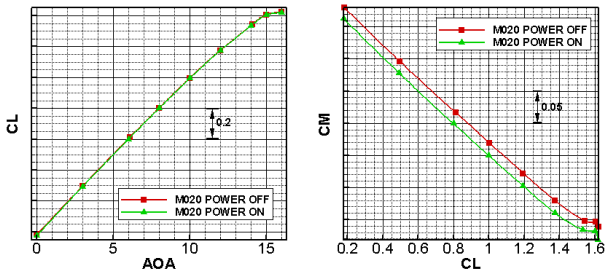

Fig. 16. Jet flow influences to the aircraft life and moment characteristics at *M*=0.20

6 Conslusions

In this paper, flow influences to civil wing-mounted aircraft aerodynamic characteristics were analyzed by using the numerical simulation method. Wing-mounted civil aircraft engine jet flow interferes the local flow field certainly, the aerodynamic characteristics have some changes. There are following:

(1) Jet flow affects wing flow field slightly. Just on the lower wing surface at the pylon neighboring regions have certain interference.

(2) Jet flow reduces the lift. When *M*= 0.785, in cruise angle (about 2 °), *CL* presumably reduces about 2.5%; *M* = 0.20, *a* = 3 °, *CL* reduces about 1%.

(3) Jet flow makes aircraft moment decreased. When *M* = 0.785 in cruising state (*CL*=0.55), *CM* decreases about 6%; *M* = 0.20, CL=0.6, *CM* decreases about 25%. No significant change for moment line slope.

References

[1] Wang Zhidong. Wing-mounted engine influences to wing design analysis [J]. Civil Aircraft Design And Research. 1997,2:19-27

[2] Aircraft Design Manual [M]. 2005:507-522

[3] Li Jie, Li Fengwei, E Qin. Numerical simulation of transonic flow over wing-mounted twin-Engine transport aircraft [J]. Journal of Aircraft, 2000, 37(3): 469-478.

[4] Tan Zhaoguang , Chen Yingchun , Li Jie . Numerical simulation method for the powered effects in airframe/propulsion integration analysis [J]. Journal of Aerospace Power. 2009,8:1766-1772

[5] Hirose N, Asai K, Ikawa K. Transonic 3-D Euler analysis of flows around fan-jet engine and T.P.S. (Turbine Powered Simulator) [R], NAL-TR-1045, 1989.

Copyright Statement